

Deep Space Relay Terminals for Mars Superior Conjunction

Julian C. Breidenthal,¹ Mark C. Jesick², Hua Xie³, and Chi-Wung Lau⁴
Jet Propulsion Laboratory, California Institute of Technology, Pasadena, California 91109, USA

The Sun periodically blocks direct communication between the Earth and Mars, creating a need for a relay when missions have a critical need for communication during these times. We examined several approaches based on optical or radio-frequency relays placed in deep space between the Earth and Mars, exploring multiple possible placements of relays, including periodic orbits in the Sun-Earth and Sun-Mars rotating frames, and eccentric, sun-centered orbits. L4 and L5 long-period orbits in the sun-Mars system provide suitable communications geometry continuously for very long durations. In such an orbit, a deep space relay terminal with two 50 cm optical telescopes and two 75 cm Ka-band dish antennas, along with associated receivers and transmitters, would be capable of supporting Mars superior conjunctions with an optical data rate of 28 to 44 Mbps for return links, and 30-36 Mbps in the forward direction. The relay should use efficient, low-noise optical detectors, such as appropriately cooled Avalanche Photo Diode or Superconducting Nanowire Single Photon Detectors, to achieve these data rates. The single relay discussed in this study might have additional value beyond communications, providing a synergistic platform for solar observation, solar wind observation, gravitational studies, the search for near-earth asteroids, or a navigational beacon.

I. Nomenclature

<i>APD</i>	=	Avalanche Photo Diode
<i>AU</i>	=	Astronomical Unit
<i>BWG</i>	=	Beam Waveguide
<i>bps</i>	=	bits per second
<i>cps</i>	=	counts per second
<i>CRTBP</i>	=	Circular-Restricted Three-Body Problem
<i>DE</i>	=	Detection Efficiency
<i>DRO</i>	=	Distant Retrograde Orbit
<i>DSRT</i>	=	Deep Space Relay Terminal Concept
<i>DTE</i>	=	Direct to Earth
<i>EIRP</i>	=	Effective Isotropic Radiated Power
<i>MLO</i>	=	Mars Leading Orbit
<i>MTO</i>	=	Mars Trailing Orbit
r_0	=	Fried parameter
<i>RF</i>	=	Radio Frequency
<i>SEP</i>	=	Sun-Earth-Probe [angle]
<i>SNSPD</i>	=	Superconducting Nanowire Single Photon Detector
<i>W</i>	=	Watt

¹ Systems Engineer, Communication Architectures Research Section, Senior Member.

² Mission Design Engineer, Mission Design and Navigation Section.

³ Telecommunications Engineer, Communication Architectures Research Section.

⁴ Telecommunications Engineer, Communication Architectures Research Section.

II. Introduction

When the Sun periodically blocks communication between the Earth and Mars, the duration of blockage can be substantial, ranging from days to weeks depending on the communication system's sensitivity to pointing close to the sun. Some missions have a critical need for communication during these times, notably manned missions to Mars contemplated by NASA and other parties.

This need raises the question as to which communications architectures might provide continuous communication despite blockage by the Sun, with sufficiently high performance and in a cost-efficient manner. The mass and size of the relay terminals, and the launch energy requirements associated with placing relay terminals in deep space, are significant factors in both the cost and performance of the resulting communication system. We examined several approaches based on a single optical or radio-frequency relay placed in deep space between the Earth and Mars, positioned so that the lines of communication avoid the close proximity to the Sun that would cause solar emission, corruption of the signal by the solar corona, or absorption by the Sun itself to inhibit communication. The resulting inflected communication path permits all terminals of the communication path to point well away from the Sun, while keeping the relay close enough to the end terminals to achieve the desired data rates.

In particular, we sought solutions that can provide data rates between 10 Mbps and 250 Mbps communication in the return direction, and between 3 Mbps and 50 Mbps in the forward direction, consistent with working requirements expressed by NASA. These ranges of data rates apply to Mars at maximum distance from the Earth, in the 2030-2040 time frame.

The single notional Deep Space Relay Terminal (DSRT) we discuss in this study might have value beyond providing communication during superior conjunction. The relay could provide a platform for solar observation, solar wind observation, gravitational studies, the search for near-earth asteroids, or a navigational beacon. The unique off-Earth location offered by the relay may enhance these applications by providing additional viewing directions or an additional measurement location to complement measurements made from Earth. The relay may also increase data return from Mars, by providing a second communication path to augment the direct path. One mechanism of data return increase results from the fact that both Mars and the relay will periodically experience closest approach to the Earth, but at different times. Closest approach reduces the communication difficulty, and depending on a number of details, may raise the data rate possible between Earth and Mars. Having both Mars and the relay experience closest approach in succession extends the length of time during which at least one is close to the Earth, and therefore the duration for which the highest data rate is possible. A second mechanism is a difference in times of eclipse between Earth and the relay, as seen from a terminal on Mars, or very near to Mars. At times, the relay will be in view when the Earth is not, extending the potential communication time for a near-Mars terminal. Finally, a single relay might eventually be combined with other relays to form a multi-hop network in deep space, resulting in a higher possible data rate¹.

III. Notional Communication Terminal Characteristics

A. Space Terminal Near Mars

We assumed that a space terminal at Mars would be as described in a companion article², that is, an Areostationary Mars-orbiting relay carrying a Ka-band (32 GHz) radio system with 940 W transmit power and a 6 m dish antenna for the return link, and capable of receiving a Ka-band (34.3 GHz) forward link. The Areostationary relay also carries a 50 cm optical telescope with three 15 W laser transmitters at 1550 nm, operating in parallel to provide the optical return link. We assumed that the detectors for the forward optical link are the same type as for the Deep Space Relay terminal discussed below.

B. Deep Space Relay Terminal

We sought to keep the deep space relay terminal small, to facilitate its launch and to moderate cost. For this reason we selected a 75 cm dish antenna for Ka-band return and forward links, and a 94 W Ka-band (34.3 GHz) transmitter. Following the system described in a companion article², we assumed the Areostationary terminal at Mars transmits from a 6 m dish antenna, with 940 W at 32 GHz toward the relay. We patterned other radio characteristics after the Mars Reconnaissance Orbiter (MRO), as detailed in Table 1.

Also in the quest for a small relay terminal, we initially examined optical link performance on the space-to-space link assuming a 10 cm aperture, and found that it could not satisfy an illumination constraint for the Areostationary relay; this reasoning is described further below. Next we examined performance with a 22 cm aperture, and though the illumination constraint could be satisfied, the relay performance was drastically lower than the direct-to-Earth (DTE) link from Mars, which would probably introduce operational difficulties and is therefore inconsistent with the purpose of having a DSRT. Therefore we assumed a 50 cm optical aperture, equipped similarly to the Areostationary relay: having three 15 W transmitters operating in parallel at 1064 nm wavelength. This enabled a return relay data rate somewhat less than the DTE optical link near superior conjunction, but still roughly comparable. However, a 22 cm aperture might be found sufficient if a substantial decrease in data rate can be tolerated during the conjunction.

Table 1: Additional Radio Link Parameters based on MRO

Relay-Mars Return Link		Relay-Mars Forward Link	
Coding Threshold for Turbo (8920, 1/6) (dB)	-0.1	Coding Threshold for Turbo (8920, 1/6) (dB)	-0.1
Margin (dB)	3	Margin (dB)	3
Modulation Index (rad)	1.045	Modulation Index (rad)	1.045
Mars Areostationary Terminal (Transmit)		Relay Terminal (Transmit)	
Antenna efficiency (%)	55	Antenna efficiency (%)	55
Transmit circuit and pointing loss (dB)	-3	Transmit circuit and pointing loss (dB)	-3
Axial Ratio	1	Axial Ratio	1
Relay Terminal (Receive)		Mars Areostationary Terminal (Receive)	
Antenna Efficiency (%)	55	Antenna Efficiency (%)	55
Receive circuit and pointing loss (dB)	-3	Receive circuit and pointing loss (dB)	-3
Axial Ratio	1	Axial Ratio	1
Noise figure	1.56	Noise figure	1.56
System Noise Temperature (K)	270	System Noise Temperature (K)	270

The relay would be expected to provide links both to Earth and Mars. To maximize system-level commonality we assumed that the Earth links would use a second instance of the equipment provided for the Mars links. That is, the relay would have two 50 cm optical telescopes, and two 75 cm Ka-band dish antennas, with corresponding transmitters and receivers.

We faced a significant question as to what optical detector capability is applicable to spacecraft optical systems. This is a rapidly evolving area of research, and a premise of this study is a time frame 15-20 years in the future. While we cannot perfectly predict what capabilities will be available at that time, we provide here observations based on recent research activity.

Current system-level optical communications experiments applicable to deep space have emphasized return data rate capability, and although some uplink capability is provided, it is known to be limited compared to downlink capability. In the cases we are aware of, the space-based optical detectors are avalanche photodiodes (APD), sometimes cooled below ambient temperature. However, the best Earth-based detectors in this wavelength range are more efficient, faster, and less noisy, specifically the superconducting nanowire single photon detectors (SNSPD) cooled to cryogenic temperatures. This situation primarily reflects a priority choice regarding deployment of limited research funds within particular experiments that did not need to prove high data rates for the forward link. Therefore we believe it would be unduly pessimistic to assume the spacecraft detectors would be the APD detectors currently in use.

We reviewed some of the literature as to the capabilities of APD and SNSPD detectors, and found a number of recent advances preparing detectors for potential space applications, both APD and SNSPD, based on several possible base materials. A snapshot of some of the types of detectors under investigation appears in Table 2. Several of these demonstrated detection efficiency (DE) in the 50-90% range, reset times and timing jitter consistent with forward data rates of tens of Mbps or more, and dark count rates between 0.01 and 150,000 counts per second. Accordingly, we adopted two potential detector types for comparison, a hypothetical APD with 60% DE and 150 kcps dark count, and a hypothetical SNSPD with 80% DE and 3 cps dark count. We later found that the higher dark count associated with the APD is not a significant obstacle at the data rates we considered.

Cooling of space-based detectors is a significant issue, but has been under development for some time. Long lifetime of cryocoolers has been demonstrated by Narasaki et al.³ and several others up to about ten years, and temperatures ranging from 80 K to 0.05 K have been achieved in a number of systems suitable for space use^{4,5,6,7,8,9,10}.

In particular, the James Webb Space Telescope is planned to carry a cryocooler^{11,12} for the Mid InfraRed Instrument (MIRI) capable of removing 55 mW of heat at 6 K temperature for bus power below 500W. The lifetime for the telescope as a whole is expected to be between 5 and 10 years¹³.

Again, both detectors and coolers are areas of active research, and we do not attempt here to forecast the exact capabilities that will be available in 2030. However, given the substantial interest in the two areas, we believe it is likely that both APD and SNSPD detectors, cooled to sufficiently low temperatures, will be feasible in that time frame. We should note that due to different operating temperatures, and the consequent differences in cryocooler weight and power consumption, either the APD or the SNSPD detectors could enable a more beneficial solution when trades between various component sizes, e.g. telescope and cryocooler, are considered in the full system context. Such a trade, however, would require detailed knowledge of equipment characteristics that is not yet available.

C. Earth Terminals

We assumed NASA Deep Space Network 34m Beam-Waveguide (BWG) antennas for Ka-band forward and return links to the DSRT.

We assumed a single 8 meter hybrid RF-optical telescope with cryogenically-cooled photon counting detectors as previously reported¹⁴, for return link capability from the relay. For the forward link, we experimented with multiple arrangements of ground transmitters, and found that 15 one-kilowatt beams, each beam with a beam waist of 1.56 cm (corresponding to 40 microradians beam divergence) was capable of providing a forward link capability comparable to the return capability. Multiple beams are used on the forward link to reduce the effect of divergence introduced by turbulence in the Earth's atmosphere¹⁵, and the beam waist is kept smaller than the Fried parameter r_0 to ensure coherence across each beam. It may be possible to reduce beam divergence further by increasing the beam waists, and thereby reduce the transmitter power needed, though we did not reach a conclusion on that topic in the course of this study. We assumed the Earth optical terminals were located at Goldstone, California for definition of atmospheric characteristics.

Table 2. Characteristics of some recently reported optical detectors.

Material	Type	Super-conducting Transition Temp (K)	Typical Operating Temp (K)	Detection Efficiency (%)	Dark Count (cps)	Reset Time (ns)	Timing Jitter (ps)	Reference
MgB ₂	SNSPD	39	4.2	4	...	Shibata et al 2013 ¹⁶
MoGe	SNSPD	7.36	0.25 to 2.5	> 20	<500	9	69-187	Verma et al 2014 ¹⁷
MoSi	SNSPD	5.2 - 7.5	0.7 - 3.0	87	3 - 70	50 - 120	76 - 120	Bannerjee et al 2017 ¹⁸ Brussieres 2017 ¹⁹ Korneeva et al 2014 ²⁰ Verma et al 2015 ²¹
NbN	SNSPD	16	1.7 - 2.9	56	95000	9	~30	Bellei et al 2013 ²²
NbSi	SNSPD	2	0.3	>80 pred.	< 1	< 1	...	Dorenbos et al 2011 ²³
WSi	SNSPD	3.7 - 5	0.12 - 2.0	93	0.01 - 10.0	40	150	Marsili et al 2013 ²⁴ Marsili et al 2013 ²⁵
HgCdTe	APD	...	77	50 - 70	150000	8	~900	Kraniak et al 2016 ²⁶
Si	APD	85000	0.6	120	Kraniak et al 2016 ²⁶
TaN	SNSPD	6-10.5	0.6-2.0	>50	10 ² -10 ⁴	Engel et al 2012 ²⁷

IV. Communication Constraints

A. Potential Relay Positions

We considered some hypothetical relay locations for initial system sizing, as depicted in Figure 1. We found that locations B, C, and D would lead to either significantly lower data rates, or to significantly larger and probably impractical relay terminals. That is a consequence of the relative difficulty of placing large apertures in space, as opposed to the Earth where a large aperture is practical and can make up for smaller space apertures. Thus, we prefer to arrange the communication distance from relay to Mars to be much smaller than the communication distance from relay to Earth. Location E satisfies this principle, and could provide high data rate with reasonable apertures, but would require a multi-hop solution to solve the solar conjunction issue and would therefore be more expensive, but not necessarily proportionally so compared to the data rate advantages¹. However we chose to avoid the multi-hop solution for this study.

Simultaneously, consideration of realistic orbit types, discussed further below, led to an awareness of a family of good solutions in the vicinity of location E. Therefore we chose to focus on that region as the best approximate location for the relay.

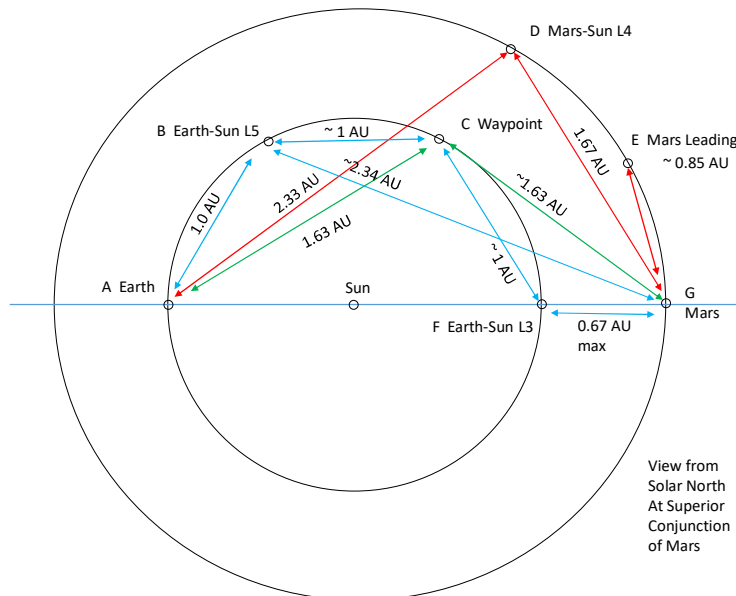


Figure 1. Potential Relay Positions. (A) Earth; (B) Earth-Sun Lagrangian Point 5; (C) A waypoint in a sun-centered orbit of about Earth’s diameter; (D) Mars-Sun Lagrangian Point 4; (E) A Mars-Leading Orbit; (F) Earth-Sun L3; and (G) Mars.

B. Solar Exclusion Zone

Solar illumination disturbs optical telescopes, both from the standpoint of scattered light in Earth’s atmosphere, and from the standpoint of safety for the telescope against heat from direct solar illumination. Recent experiments using the Hale Telescope at Palomar Observatory adopted a limit of 20 degrees for sun-Earth-probe (SEP) angle for this reason, although designs have been tested to enable SEP down to 3 degrees²⁸. Our opinion, informed by discussions with a prospective telescope manufacturer, is that this limit might be reduced perhaps as low as 10 degrees, but it is presently unknown whether it is possible reduce it to 5 degrees. For the distances we contemplate, the data rate capacity on the relay-Mars link depends roughly on the inverse-square of the distance between the relay and Mars, and therefore on the SEP of the Earth-relay link. We adopted SEP 10 degrees as the reference for this study, although smaller values may be possible and would serve to increase the data rate achievable.

At RF, SEP limits on the Earth-relay link are set by increased system noise temperature and scintillation from the solar wind. At X-band the practical limit on SEP is around 2.2 degrees, or 1.2 degrees at Ka-band^{29,30}.

The relay-Mars links from locations C, D, and E are operated at large enough angles away from the Sun that they do not need additional solar exclusion constraints.

C. Beacon Illumination Intensity

The present deep space optical communication architecture planned for Mars provides a beacon to space terminals, to assist the spacecraft with acquisition of the forward link, and to overcome spacecraft attitude disturbances³¹. This is not the only possibility; other architectures³² avoid the need for the beacon, but may involve extra expense for equipment to orient the optical terminal very precisely. However, if a beaconless architecture proved to be advantageous, obviously the illumination intensity constraint could be relaxed, allowing an opportunity to choose a smaller relay terminal if desired, with concomitant lower data rate capacity. Nonetheless, in our analysis a larger terminal driven by beacon illumination provided a higher data rate that appears to be closer to the operational desires.

With the current design of the Deep Space Optical Terminal, the beacon illumination level needed³³ is about 4 pW/m². This is largely independent of aperture size on the illuminated end of the link, because larger receiving apertures require finer pointing, and therefore less noisy information about the direction of illumination, canceling the benefit of larger aperture in net. The requirement on illumination level leads to a constraint on minimum effective isotropic radiated power as a function of communication distance, and therefore to a constraint on relay aperture and power. This constraint may be evaluated with the help of Figure 2, which depicts the communication distance at which the illumination constraint is met, for various combinations of transmitter power and aperture diameter. A minimum distance of 0.85 AU is needed to satisfy the solar exclusion constraint discussed further below, which leads to a conclusion that very high transmitter power, >100 W would be needed to enable a 5 cm relay aperture to satisfy the illumination constraint. The aperture we adopted for the relay, 50 cm, can satisfy the illumination constraint with any power greater than 1 watt. Our assumed power is higher, to enable a satisfactory forward link data rate.

D. Data Rate Balance

The data rate into and out of the relay must be balanced long term, so that the Earth links do not become bottlenecks themselves. All of the Earth links we describe here satisfy that constraint on the average. However we should note that the optical link data rates on the Earth links vary substantially on a diurnal basis due to solar illumination and weather. Therefore approximately a day's worth of data storage is needed in the relay to balance data rate. Clare et al. 2016 found that more storage may be required depending on latency and continuity goals³⁴.

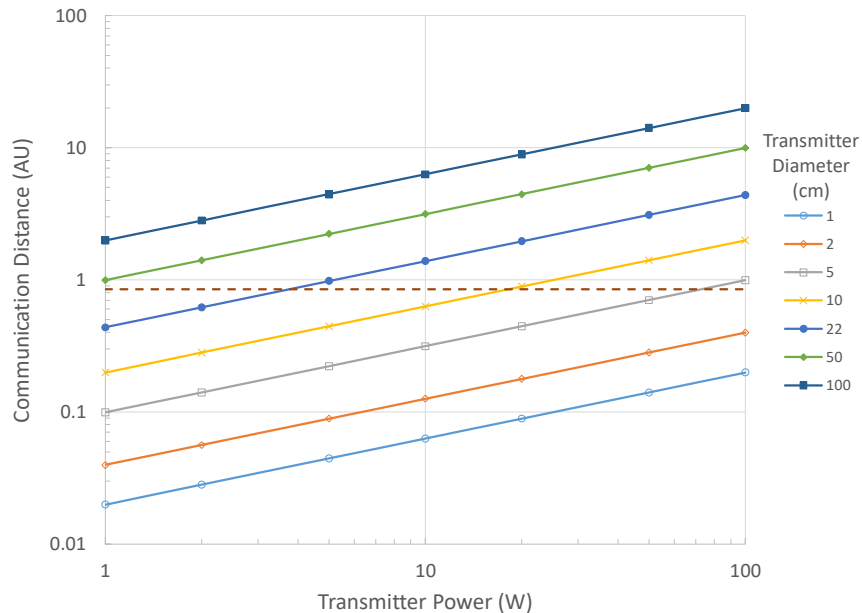


Figure 2. Communication distance satisfying illumination constraint. The dashed line represents the solar exclusion zone $d_{min} = 0.85$ AU corresponding to SEP=10 degrees.

V. Relay Orbit Selection

A. Geometric Constraints

The telecommunications constraints described above imply geometric constraints on the deep space relay spacecraft orbit. The solar exclusion zone established by the minimum SEP angle defines a cone with its apex at the Earth and centerline coincident with the Earth-sun line, within which the relay spacecraft must not pass during Earth-Mars solar conjunction periods. The maximum distance during relay communications with Mars-based assets defines a Mars-centered sphere within which the relay spacecraft must remain during solar conjunction periods. Therefore, we desired to find orbits that situate the relay spacecraft outside the solar exclusion zone but within the Mars communication sphere and do so during multiple solar conjunction periods. Figure 3 shows a planar view of these constraints.

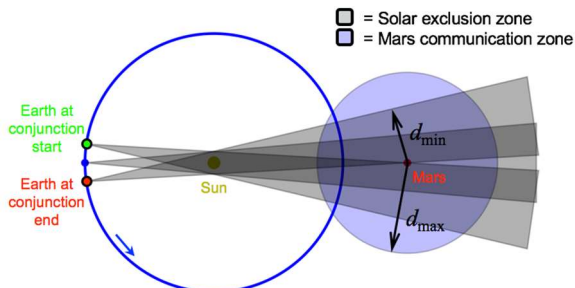


Figure 3: Geometric constraints (sun-Mars rotating frame).

Table 3: Minimum Mars-spacecraft distance

Minimum SEP angle	Minimum distance
5 deg	0.43 AU
10 deg	0.85 AU
15 deg	1.22 AU
20 deg	1.54 AU

* Assumes $r_{\text{Earth}} = 1.0$ AU and $r_{\text{Mars}} = 1.5$ AU.

The solar exclusion zone imposes a minimum distance requirement on the spacecraft trajectory if the relay is to be visible to Earth and Mars during an entire solar conjunction period. Assuming a circular, coplanar solar system, and a coplanar relay spacecraft orbit, the minimum distance to Mars is a function of the minimum SEP angle only. At the commencement of the solar conjunction period, any spacecraft “ahead” of the Earth-Mars line will be outside the solar exclusion zone, and any relay spacecraft “behind” the Earth-Mars line must be at least a distance d_{min} away from Mars to be outside the solar exclusion region (Figure 3). Similarly, at the termination of the solar conjunction period, any spacecraft ahead of the Earth-Mars line must have a Mars range of at least d_{min} , and any spacecraft behind the Earth-Mars line will be outside the solar exclusion zone. Therefore, if the Mars-spacecraft distance remains greater than d_{min} during the entire period, it is guaranteed to provide a continuously visible Earth-Mars communications relay. Table 3 shows the minimum distance for select values of the minimum SEP angle.

B. Orbit Type Selection

An orbit satisfying the aforementioned geometric constraints must pass at least once through the visible portion of the communications zone, and either remain in the visible communications zone for an extended duration, or re-enter it every Earth-Mars synodic period. Many trajectories could place the spacecraft in the communications zone for only one solar conjunction period, but such a single-use relay would likely not be cost-effective unless it was also repurposed for another mission. Therefore, repeatability of the relay geometry is desired, so periodic orbits are considered; and because the communication endpoints are Mars and Earth, periodic orbits are considered in the sun-Mars and sun-Earth systems. The circular-restricted three-body problem (CRTBP) is used to model spacecraft dynamics in the initial orbit search. We examined 38 periodic orbit families in both the sun-Mars and sun-Earth systems (every family available in the orbit database of JPL’s Mission Operations and Navigation Toolkit Environment software), including libration point, secondary-centered, and resonant orbit families.

Table 4 shows the evaluation of each orbit family in the sun-Mars system. Due to this system’s low mass ratio of $\mu_{\text{Mars}}/(\mu_{\text{Sun}} + \mu_{\text{Mars}}) \approx 3.2 \times 10^{-7}$, orbits far from Mars are only weakly affected by its gravity and thus are essentially sun-focused ellipses in a non-rotating reference frame. Many families contain members who satisfy the spatial constraints, but only two families also satisfy the temporal constraints. Some well-known periodic orbit families at the collinear libration points (e.g. L_1 Lyapunov and L_2 halo) remain so near to Mars that the entire family exists within the solar exclusion zone and thus no individual orbit satisfies the problem’s geometric constraints. Other families, like Mars’s distant retrograde orbits (DROs), do include orbits that reach outside of the exclusion zone, but the periods of

these DROs are essentially equal to Mars’s heliocentric orbit period and not useful for multiple solar conjunction periods. The only families satisfying all geometric and temporal constraints are the L_4 and L_5 long-period families. These so-called Trojan orbits are planar, circumnavigate one triangular equilibrium point, and, in the sun-Mars circular-restricted system, have an orbital period over 1100 Earth years. Although these orbits do not remain permanently in the communications zone, the orbital period is so long that a spacecraft following such an orbit can remain in the communications zone well past the spacecraft’s expected lifespan. L_4 or L_5 long-period orbits in the sun-Mars circular-restricted system oscillate about their respective triangular equilibrium point and maintain a heliocentric radius near that of Mars. As can be seen in the example L_4 long-period orbit of Figure 4, the orbit, with a period of 1115 Earth years, proceeds clockwise around the libration point, remains ahead of Mars in its orbit, and exhibits a radial deviation so small it is not discernable on this scale. A larger orbit in this family that passes nearer to Mars would be chosen for the relay spacecraft.

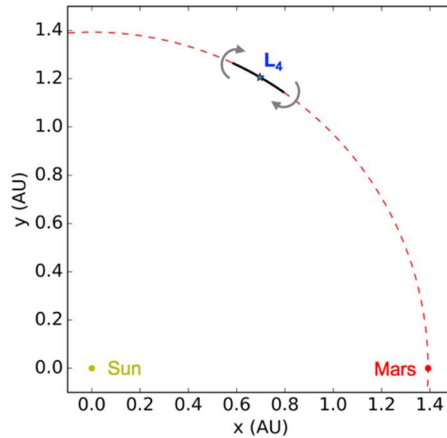


Figure 4: Example L_4 long-period orbit in sun-Mars CRTBP (rotating frame).

A similar result follows for orbit families in the sun-Earth system. All families contain orbits that escape the solar exclusion zone, but few orbits enter the Mars communications zone. Of those that do, none re-enter it in a time period commensurate with the Earth-Mars synodic period, and only the L_4 and L_5 long-period (Trojan) orbits enable a spacecraft to remain in the communications zone for extended time periods. Because these orbits in the sun-Earth system exhibit greater Mars-spacecraft distances than their analogs in the sun-Mars system, the sun-Earth periodic orbits are not considered in this investigation but are certainly worthy of future study, because these orbits allow significantly reduced Earth-departure energy and relay orbit-insertion costs through the use of a multi-revolution outbound transfer.

Additionally, eccentric solar orbits with a perihelion of 1 AU with no periodicity in the CRTBP were investigated, but, as expected, could provide relay communications for only one or two consecutive Earth-Mars solar conjunction periods. Placing multiple relay spacecraft along this type of orbit could provide a viable long-term solution, but, since this study focuses on a single-spacecraft architecture, this topic is not pursued here.

C. Mars Leading Orbits

When the CRTBP model is upgraded to a multibody ephemeris model, no truly periodic orbits exist because the solar system geometry does not repeat exactly. Additionally, the eccentricity of Mars’s orbit (~ 0.1) imparts a per-revolution oscillation in the spacecraft’s angular offset from Mars. To distinguish between the periodic orbits of the CRTBP and the quasi-periodic orbits of the ephemeris model, orbits in the latter model that lead Mars will be referred to as Mars leading orbits (MLOs). The equivalent of L_5 long-period orbits in the ephemeris model will be called Mars trailing orbits (MTOs). Figure 5 shows an example MLO propagated for one Mars year; its shape is due almost entirely to Mars’s orbital eccentricity. MLOs drift slowly enough that a spacecraft on an MLO can remain within the visible communication zone for decades, well past the expected lifetime of the vehicle. In general, the closer an MLO begins to Mars, the faster it will drift away.

Table 4: Sun-Mars periodic orbit family evaluation

Family	Extends beyond solar exclusion zone*	Enters visible comm zone†	Remains in visible comm zone for extended period	Re-enters visible comm zone synodically
L ₁ Axial	No	—	—	—
L ₁ Halo‡	No	—	—	—
L ₁ Lyapunov	No	—	—	—
L ₁ Vertical	Yes	Yes	No	No
L ₂ Axial	Yes	Yes	No	No
L ₂ Butterfly‡	No	—	—	—
L ₂ Halo‡	No	—	—	—
L ₂ Lyapunov	No	—	—	—
L ₂ Vertical	Yes	Yes	No	No
L ₃ Axial	Yes	Yes	No	No
L ₃ Halo‡	Yes	No	—	—
L ₃ Lyapunov	Yes	No	—	—
L ₃ Vertical	Yes	Yes	No	No
L ₄ Axial	Yes	Yes	No	No
L ₄ Short	Yes	Yes	No	No
L ₄ Long	Yes	Yes	Yes	—
L ₄ Vertical	Yes	Yes	No	No
L ₅ Axial	Yes	Yes	No	No
L ₅ Short	Yes	Yes	No	No
L ₅ Long	Yes	Yes	Yes	—
L ₅ Vertical	Yes	Yes	No	No
Dragonfly‡	No	—	—	—
Distant Retrograde	Yes	Yes	No	No
Distant Prograde	No	—	—	—
Low Prograde§	No	—	—	—
Resonant 1:1	Yes	Yes	No	No
Resonant 1:2	Yes	Yes	No	No
Resonant 1:3	Yes	Yes	No	No
Resonant 2:1	Yes	Yes	No	No
Resonant 2:3	Yes	Yes	No	No
Resonant 3:1	Yes	Yes	No	No
Resonant 3:4	Yes	Yes	No	No

* Minimum SEP angle of 5 deg.

† Maximum Mars range of 1 AU.

‡ Includes northern and southern families.

§ Includes eastern and western families.

A spacecraft bound for an MLO departs Earth and follows an elliptical outbound transfer similar to a standard Earth-Mars transfer, except the spacecraft aims for a destination ahead of Mars in its heliocentric orbit (Figure 6). At the end of the transfer, the spacecraft performs a propulsive maneuver to assume the position and velocity that Mars would have at that point in Mars's orbit. After the orbit insertion maneuver, the spacecraft nominally requires no propulsive maneuvers since it will maintain for decades nearly the same position relative to Mars, depending on their initial angular offset. The minimum possible angular offset between the sun-Mars and sun-spacecraft lines is dictated by the relay spacecraft's telecom architecture. This angle, in turn, defines the closest possible points along Mars's orbit where a relay spacecraft may reside. These two points represent Mars's position in the future (for MLOs) and the past (for MTOs). Because of Mars's orbital eccentricity, the forward and backward temporal offsets are not equal in general, and depend on the position of Mars at orbit insertion.

To locate optimal time periods for Earth departure and MLO arrival, the Earth departure energy and orbit insertion velocity impulse are computed for a range of Earth departure and MLO arrival dates (the same process would work equally well for MTOs). For each launch and arrival date pair, Lambert's problem is solved for the transfer between Earth and the MLO insertion location. Transfers to MLOs are similar to Earth-Mars transfers but are unique and effectively represent a different Earth-Mars phasing. The characteristic contours (e.g. Earth departure energy) of MLO transfers are therefore shifted and warped relative to Earth-Mars transfers, but become more similar as the magnitude of the angular offset decreases. Figure 7 shows twice the Earth departure energy (C_3) and the orbit insertion impulse magnitude (ΔV) for transfers that depart Earth in 2033 and target an MLO with an initial angular offset of 10 degrees

relative to Mars. The minimum C_3 and ΔV during this launch opportunity are $13.5 \text{ km}^2/\text{s}^2$ and 2.4 km/s , respectively. The outbound transfer associated with the minimum ΔV requires a flight time of about seven months. Favorable dates derived from the data of Figure 7 can be used for the selection of a multi-week launch period.

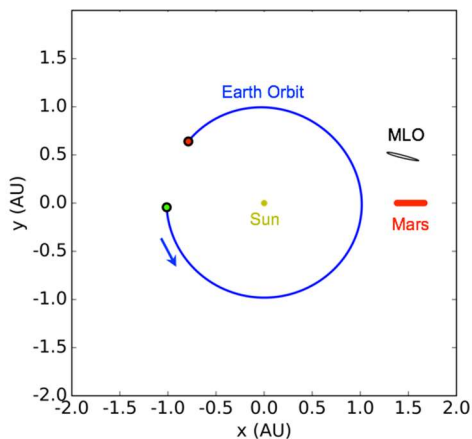


Figure 5: Example MLO in ephemeris model (sun-Mars rotating frame).

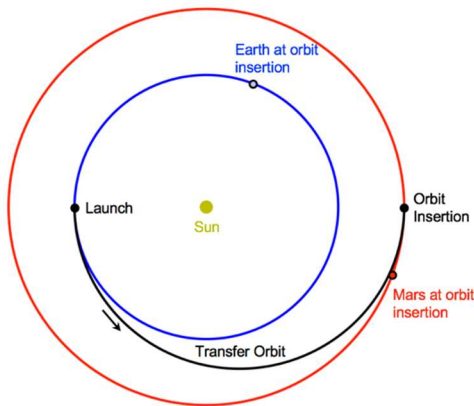


Figure 6: Outbound transfer and MLO insertion.

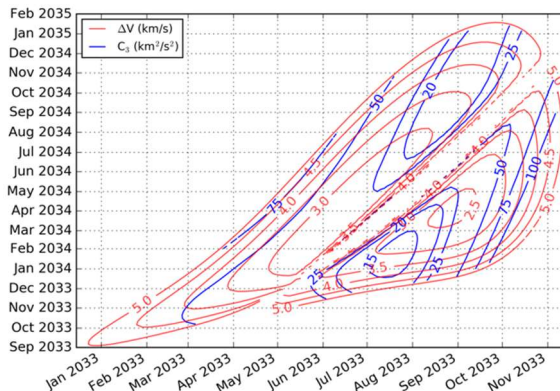


Figure 7: Twice Earth departure energy and orbit insertion impulse.

VI. Estimated Communications Performance

We estimated achievable data rates for the range of terminal sizes and communications distances associated with Mars superior conjunction, considering various communications constraints including provision of sufficient optical power toward the Mars orbiting relay to allow it to acquire precise optical pointing needed for communication. The relay orbit used was a MLO launched January 1, 2029, arriving in the relay orbit on October 1, 2029. This orbit enables support of superior conjunctions beginning with the conjunction of May-June 2030.

A. Radio Frequency Links

We evaluated the performance capability of the RF link between the DSRT and the Mars Areostationary orbiter using RF link analysis embodied in the JPL Telecommunications Forecaster Predictor software. The relay orbit was that described above, and the Areostationary orbiter being in close proximity to Mars could be considered to be at the center of Mars with sufficient accuracy for the purpose of link evaluation.

The resulting Ka-band data rates as a function of time appear in Figures 8 and 9. The times of interest to the analysis consist of the period after the relay orbiter achieves its final orbit 17 January 2030. For the return link a maximum data rate of 185 kbps and a minimum data rate of 127 kbps can be achieved. The forward link achieves a maximum data rate of 21 kbps and minimum data rate of 14 kbps.

For the Earth-DSRT link, we checked the data rate balance criterion by scaling from the results in a companion article². There, two 34-m BWG arrayed antennas are shown to be capable of 50 Mbps return from a Mars Areostationary relay with a 470 W transmitter data rates and a 6 meter dish antenna, at Mars maximum range. Scaling to our assumed Ka-band relay terminal, 75 cm dish antenna and a 94 W transmitter, the capability is 156 kbps return on the Earth-DSRT link using two 34m BWG antennas. In the forward direction, two arrayed 34-m BWG antennas transmitting 1 kW each are shown to be capable of 30 Mbps. Scaling to our assumed relay terminal, the forward link capability is 117 kbps. Thus, the Earth-DSRT links are not a limiting factor for forward links, but may be a limiting factor for the return links at times when the space-to-space data rate capacity is between 156 kbps and 186 kbps. This might justify a slightly larger Ka-band antenna or transmitter to avoid a bottleneck on the Earth link.

B. Optical Links

We evaluated the performance capability of the optical links between the DSRT, the Mars Areostationary orbiter, and Earth using the Strategic Optical Link Tool (SOLT), following the methods described by Xie et al³⁵. We included the effects of Earth atmospheric transmittance, turbulence, and solar radiance on the Earth links, and optimized the link parameters, e.g. data rate, field of view, order of pulse-position modulation (PPM), code rate, and slot width. In most cases, the optimum data rate changes many times during a view period; we reduced these variations to an average data rate by calculating the data volume resulting from a view period, and then dividing by the duration of the view period. We assumed 3 dB optical losses on all terminals, and required a 3 dB communication margin as is typical this far in advance of a mission. Additional details of the optical links are provided in Table 5.

The resulting optical data rates as a function of time appear in Figures 10 and 11. At times of superior conjunction, the DTE links achieve 150 Mbps return, and 40-45 Mbps forward. The corresponding space-to-space link data rates are 28-32 Mbps (APD), 36-44 Mbps (SNSPD) in the return direction, and 30-36 Mbps in the forward direction.

For the Earth-DSRT link, we again checked the data rate balance criterion and found in all cases that the space-to-space link is the limiting factor.

VII. Conclusion

We examined 38 periodic orbit families in both the sun-Mars and sun-Earth systems including libration point, secondary-centered, and resonant orbit families. The only families satisfying all geometric and temporal constraints are the L_4 and L_5 long-period families in the Sun-Mars system, also known as Mars Leading Orbits and Mars Trailing Orbits. These orbits have periods over 1100 Earth years, allowing a deep-space relay to remain in a useful communications location well past the spacecraft's expected lifespan. Other orbits, such as Earth leading/trailing orbits and eccentric solar orbits with a perihelion of 1 AU, may be useful but were excluded from this study due to lower data rate capacity for practical relay sizing (in the case of the former), or a need for multiple spacecraft to provide a viable long-term solution (in the case of the latter).

A communication constraint to avoid pointing Earth optical terminals closer than 10 degrees to the Sun leads to a requirement that a MLO for the deep space relay be selected that is at least 0.85 AU from Mars. At that distance, the need to provide beacon illumination, combined with limitations on transmitter power, leads to a requirement for the relay optical terminal to have a diameter of at least 22 cm and preferably 50 cm. A deep space relay terminal placed in an appropriate MLO or MTO, and having two 50 cm optical telescopes and two 75 cm Ka-band dish antennas, along with associated receivers and transmitters, is capable of supporting Mars superior conjunctions with an optical data rate of 28 to 44 Mbps for return links, and 30-36 Mbps in the forward direction. The relay should use efficient, low-noise optical detectors, such as appropriately cooled Avalanche Photo Diode or Superconducting Nanowire Single Photon Detectors to achieve these data rates. The corresponding capability for the Ka-band links is 127 to 185 kbps in the return direction, and 14 to 21 kbps in the forward direction.

Table 5. Detailed Optical Link Parameters.

Link Parameter	DTE Return	DTE Forward	Relay Return	Relay Forward
Modulation and Laser				
Minimum Slot Width	0.5 ns	1 ns	0.5 ns	0.5 ns
PPM Order Optimization Range	2..128	2..128	2..128	2..128
Wavelength	1550 nm	1064 nm	1550 nm	1064 nm
Coding	SC PPM	SC PPM	SC PPM	SC PPM
Transmitter				
Average Laser Power	15 W	15 kW	15 W	15 W
Diameter or Beam Divergence	50 cm	40 μ rad	50 cm	50 cm
Optical loss	3 dB	3 dB	3 dB	3 dB
Pointing Error	1.3 μ rad	8 μ rad	1.15 μ rad	1.15 μ rad
Number of Transmit Beams	1	15	1	1
Channel				
Atmospheric Channel	Clear Sky	Clear Sky	Vacuum	Vacuum
Turbulence	Desert	Desert
Altitude	1 km	1 km
Planet Body Radiance	...	0.02 W/cm ² - sr- μ m
Detector				
Detection Efficiency, DE	80 %	60 %	60 %	60 %
Dark Count Rate	225 kcps	150 kcps	150 kcps	150 kcps
Detector Diameter	3 mm	3 mm	3 mm	3 mm
Detector Jitter	0.1 ns	0.1 ns	0.1 ns	0.1 ns
Receiver				
Diameter	8 m	50 cm	50 cm	50 cm
Focal Length	124 m	522 m	1.5	1.5
Optical Loss	3 dB	3 dB	3 dB	3 dB
Filter Bandwidth	0.17 nm	0.1 nm	0.17 nm	0.17 nm
Filter Loss	0 dB	0 dB	0 dB	0 dB
Cleanliness	1000	1000	1000	1000
Field Of View Selection Model	Analytic 90% Power	Analytic 90% Power	Analytic 90% Power	Analytic 90% Power
Required Link Margin	3 dB	3 dB	3 dB	3 dB

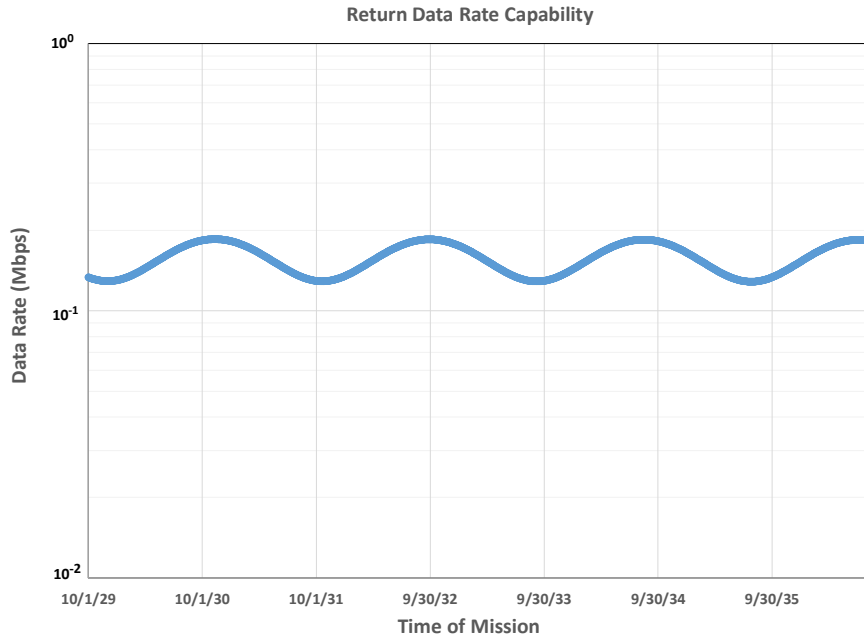


Figure 8: Ka-Band Return Link Data Rate Capability

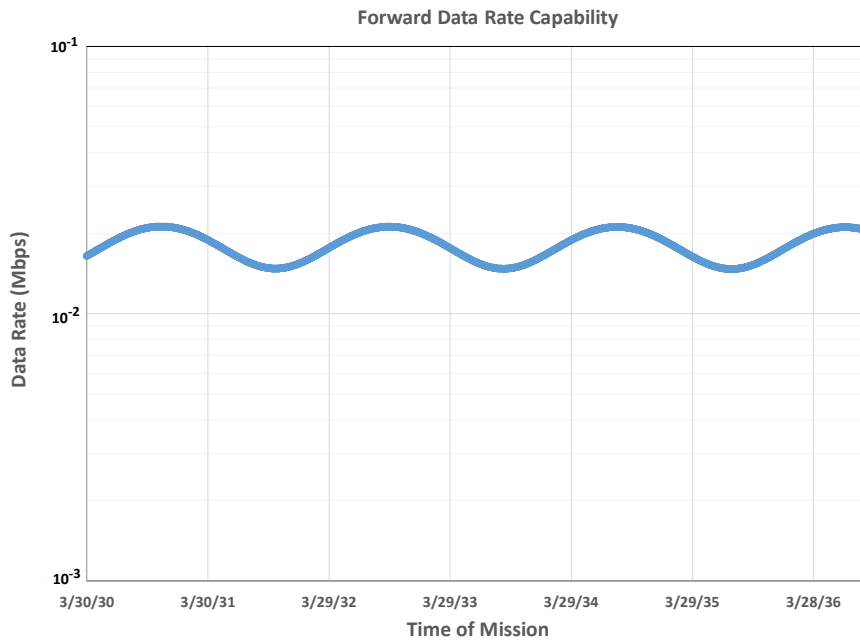


Figure 9: Ka-band Forward Link Data Rate Capability

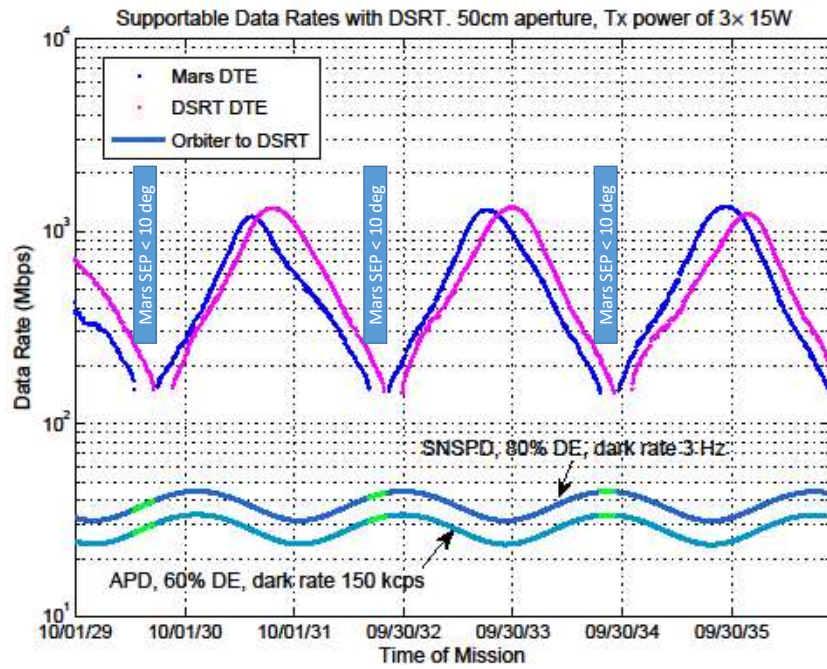


Figure 10. Optical Return Data Rate Capability.

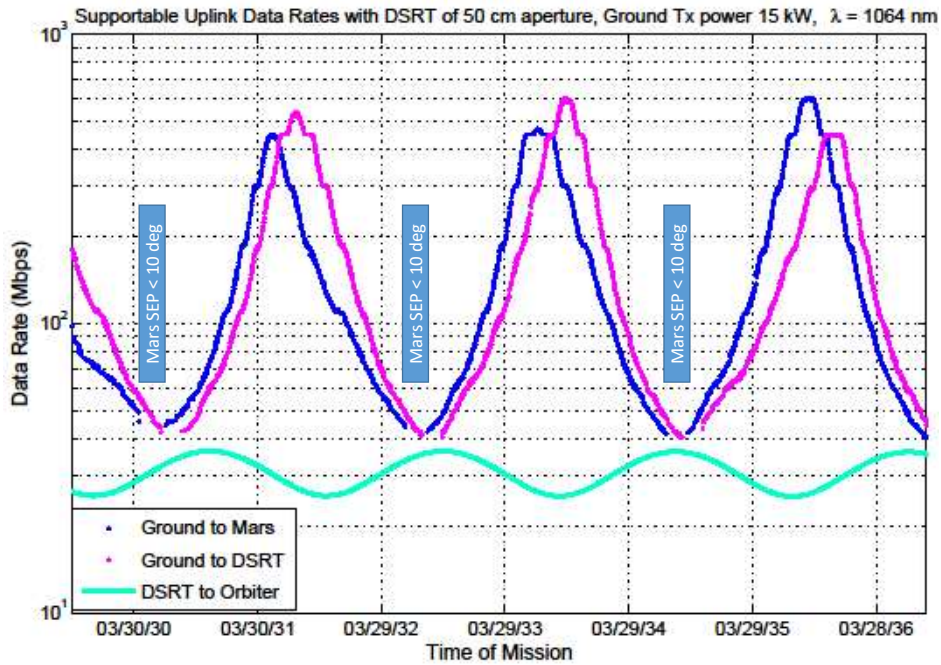


Figure 11. Optical Forward Data Rate Capability.

Acknowledgments

The work contributed by the Jet Propulsion Laboratory, California Institute of Technology, was performed under a contract with the National Aeronautics and Space Administration.

References

- [1] Breidenthal, J. C., “The Merits of Multi-hop Communication in Deep Space”, *IEEE Aerospace Conference*, Vol. 7, 00TH8484, IEEE, Piscataway, NJ, 2000.
- [2] Breidenthal, J. C., Xie, H., Lau, C.-W., and MacNeal, B., “Space and Earth Terminal Sizing for Future Mars Missions”, *AIAA Space Ops 2018 Conference*, AIAA, Washington, DC, 2018.
- [3] Narasaki, K., Tsunematsu, S., Otsuka, K., Kanao, K., Okabayashi, A., Yoshida, S., Sugita, H., Sato, Y., Mitsuda, K., Nakagawa, T., and Nishibori, T., “Lifetime Test and Heritage On-Orbit of SHI Coolers for Space Use”, *Cryocoolers 19*, International Cryocooler Conference, Inc., Boulder, CO, 2016.
- [4] Brasiliano, D.A.P., Duval, J.-M., Luchier, N., D’Escrivan, S., and Andre, J., “Development of a 3-stage ADR for Space including CCA 50 mK Characterization”, 2016.
- [5] Charrier, A., Charles, I., Rousset, B., Daniel, C., and Duval, J.-M., “Development of a 4K Pulse-Tube Cold Finger for Space Applications”, *Cryocoolers 18*, International Cryocooler Conference, Inc., Boulder, CO, 2014.
- [6] Chen L., Wu X., Liu X., Pan C., Zhou Y., and Wang J., “Numerical and experimental study on the characteristics of 4 K gas-coupled Stirling-type pulse tube cryocooler”, *International Journal of Refrigeration*, 88, Elsevier, Amsterdam, 2018.
- [7] Kirkconnell, C. S., Mulcahey, T. I., Ghiaasiaan, S. M., Conrad, T. J., and Schaefer, B. R., “Design of a 4K Hybrid Stirling/Pulse Tube Cooler for Tactical Applications”, 2012.
- [8] Marquardt, J.S., Marquardt, E.D., and Boyle, R., “An Overview of Ball Aerospace Cryocoolers”, *Cryocoolers 17*, International Cryocooler Conference, Inc., Boulder, CO, 2013.
- [9] Martin, S., Volpe, A., Vermeulen, G., Camus, P., Triqueneaux, S., Butterworth, J., D’Escrivan, S., and Tirolien, T., “Development of the Closed-Cycle Dilution Refrigerator for Space Applications”, *Cryocoolers 18*, International Cryocooler Conference, Inc., Boulder, CO, 2014.
- [10] Prouvé, T., Holmes, W., Bock, J.J., and Bradford, C., Matt., “A 1K 4He Close Cycle Loop Precooled Using a PT415 Pulse Tube for the BLISS Test Bed Cryostat”, *Cryocoolers 17*, International Cryocooler Conference, Inc., Boulder, CO, 2012.
- [11] Petach, M., Michaelian, M., Nguyen, T., Colbert, R., and Mullin, J., “Mid InfraRed Instrument (MIRI) Cooler Compressor Assembly Characterization”, *Cryocoolers 19*, International Cryocooler Conference, Inc., Boulder, CO, 2016
- [12] Petach, M., Michaelian, M., “Mid InfraRed Instrument (MIRI) Cooler Cold Head Assembly Acceptance Testing and Characterization”, *Cryocoolers 18*, International Cryocooler Conference, Inc., Boulder, CO, 2014
- [13] Greenhouse, M., “The James Webb Space Telescope: Mission overview and status”, *2nd International Conference on Space Technology*, AIAA, Washington, DC, 2011.
- [14] Charles J.R., Hoppe D.J., and Schic, A., “Hybrid RF / Optical Communication Terminal with Spherical Primary Optics for Optical Reception”, *2011 International Conference on Space Optical Systems and Applications*, IEEE, Piscataway, NJ, 2011.
- [15] Biswas, A., Hemmati, H., Piazzolla, S., Moision, B., Birnbaum, K., and Quirk K., “Deep-space Optical Terminals (DOT) Systems Engineering”, *Interplanetary Network Progress Report*, 42-183, 2010
- [16] Shibata, H., Akazaki, T., and Tokura, Y., “Fabrication of MgB₂ Nanowire Single-Photon Detector with Meander Structure”, *Applied Physics Express*, 6, 023101, 2013.
- [17] Verma, V. B., Lita, A. E., Vissers, M. R., Marsili, F., Pappas, D. P., Mirin, R. P., and Nam, S. W., “Superconducting nanowire single photon detectors fabricated from an amorphous Mo_{0.75}Ge_{0.25} thin film”, *Applied Physics Letters*, 105, 022602, 2014.
- [18] Banerjee, A., Baker, L. J., Doye, A., Nord, M., Heath, R. M., Erotokritou, K., Bosworth, D., Barber, Z. H., MacLaren, I., and Hadfield, R. H., “Characterisation of amorphous molybdenum silicide (MoSi) superconducting thin films and nanowires”, *Superconductor Science and Technology*, 30, 084010, 2017.
- [19] Brussieres, F., “Superconducting Nanowire Single-Photon Detectors for Quantum Secure Satellite Optical Communication”, *ScyLight Workshop*, ESTEC, Noordwijk, 2017.
- [20] Korneeva Y. P., Mikhailov, M. Y., Pershin, Y. P., Manova, N. N., Divochiy, A. V., Vakhtomin, Y. B., Korneev, A. A., Smirnov, K. V., Sivakov, A. G., Devizenko, A. Y., and Goltsman, G. N., “Superconducting single-photon detector made of MoSi film”, *Superconductor Science and Technology*, 27, 095012, 2014.
- [21] Verma, V. B., Korzh, B., Bussières, F., Horansk, R. D., Dyer, S. D., Lita, A. E., Vayshenker, I., Marsili, F., Shaw, M. D., Zbinden, H., Mirin, R. P., and Nam, S. W., “High-efficiency superconducting nanowire single-photon detectors fabricated from MoSi thin-films”, National Institute of Standards and Technology, Publication ID 918031, Boulder, CO, 2015.
- [22] Bellei, F., Cartwright, A. P., McCaughan, A. N., Dane, A. E., Najafi, F., Zhao, Q., Berggren, K. K., “Free-space-coupled superconducting nanowire single-photon detectors for infrared optical communications”, *Optics Express*, Volume 24, 2013.
- [23] Dorenbos, S. N., Forn-Díaz, P., Fuse, T., Verbruggen, A. H., Zijlstra, T., Klapwijk, T. M., and Zwiller, V., “Low gap superconducting single photon detectors for infrared sensitivity”, *Applied Physics Letters*, 98, 251102, 2011

- [24] Marsili, F., Verma, V. B., Stern, J. A., Harrington, S., Lita, A. E., Gerrits, T., Vayshenker, I., Baek, B., Shaw, M. D., Mirin, R. P., and Nam, S. W., “Detecting Single Infrared Photons with 93% System Efficiency”, *Nature Photonics*, September 2012.
- [25] Marsili, F., Verma, V. B., Stern, J. A., Harrington, S., Lita, A. E., Gerrits, T., Vayshenker, I., Baek, B., Shaw, M. D., Mirin, R. P. and Nam, S. W., “Detecting single infrared photons with 93% system efficiency”, *Nature Photonics Letters*, 2013.
- [26] Krainak, M. A., Yanga, G., Suna, X., Lua, W., Merritta, S., Beck, J., “Novel photon-counting detectors for free-space communication”, NASA Technical Report, 201600002949, 2016
- [27] Engel, A., Aeschbacher, A., Inderbitzin, K., Schilling, A., Il’in, K., Hofherr, M., Siegel, M., Semenov, A., and Hübbers, H.-W., “Tantalum nitride superconducting single-photon detectors with low cut-off energy”, *Applied Physics Letters*, 100, 062601, 2012.
- [28] Biswas, A., Moision, B., Roberts, W.T., Farr, W.H., Gray, A., Quirk, K., Hamkins, J., Cheng, M.K., Gin, J., Nakashima, M., Ortiz, G. G., Piazzolla, S., Liebe, C.C, and Losh, D.L., “Palomar Receive Terminal (PRT) for the Mars Laser Communication Demonstration (MLCD) Project”, *Proceedings of the IEEE*, Vol. 95, No. 10, 2007.
- [29] Morabito, D. D., “Solar corona–induced fluctuations on spacecraft signal amplitude observed during solar superior conjunctions of the Cassini spacecraft”, *Radio Science*, Vol. 42, RS3002, 2007.
- [30] Morabito, D. D., and Hastrup, R., “Communications with Mars During Periods of Solar Conjunction: Initial Study Results”, Interplanetary Network Progress Report 42-147, 2001.
- [31] Biswas, A., Hemmati, H., Piazzolla, S., Moision, B., Birnbaum, K., and Quirk, K., “Deep-space Optical Terminals (DOT) Systems Engineering”, *Interplanetary Network Progress Report*, 42-183, 2010.
- [32] Swank, A.J., Aretskin-Hariton, E., Le, D.K., Sands, O.S., “Beaconless Pointing for Deep Space Optical Communication”, 34th AIAA International Communications Satellite Systems Conference, AIAA, Washington, DC, 2016.
- [33] Farr, W., Regehr, M., Wright, M., Sheldon, D., Sahasrabudhe, A., Gin, J., and Nguyen, D., “Overview and Design of the DOT Flight Laser Transceiver”, *Interplanetary Network Progress Report*, 42-185, 2011.
- [34] Clare, L., Miles, G., and Breidenthal, J., “Optical Communications Performance with Realistic Weather and Automated Repeat Query”, *Interplanetary Network Progress Report*, 42-205, 2016.
- [35] Xie, H., Heckman, D., and Breidenthal, J., “Link Characterization for Deep-Space Optical Communications”, *Interplanetary Network Progress Report*, 42-205, 2016.